Optical Materials 144 (2023) 114275

Contents lists available at ScienceDirect

Optical Materials

journal homepage: www.elsevier.com/locate/optmat

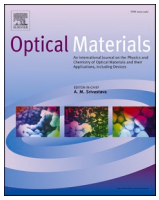

Research Article

Modeling LEDs radiation patterns for curing UV coatings inside of pipes

Alessandro Condini [a,b,*], Viktor Morozov [c], Carlo Trentalange [b], Stefano Rossi [a]

[a] Department of Industrial Engineering, University of Trento, Trento, Italy
[b] Elixe srl, Trento, Italy
[c] MPR srl, Trento, Italy

ARTICLE INFO

Keywords:
UV-Curing
LEDs
Pipelines
Radiation patterns
Organic coatings

ABSTRACT

This study investigated the use of ultraviolet light-emitting diodes (UV LEDs) for the curing of a UV protective coating on the inner surface of pipes for application in the oil and gas industry. The lamp described here comprises several 1 W LEDs mounted on linear arrays around a cylindrical support. To achieve the optimal curing of the polymeric coating on every surface point, the radiation pattern emitted by the source was simulated in both the radial and linear directions of the lamp axis. By changing the number of arrays, the spacing between LEDs and the distance from source to surface, it was possible to evaluate the best radiation pattern having less intensity variation on the pipe surface. Once the best lamp design was found, the lamp was constructed, and the actual value of irradiance was evaluated as a function of distance in the radial and linear coordinates using a radiometer.

1. Introduction

Corrosion is considered the leading cause of failures of steel infrastructures operating in harsh environments, such as oil and gas applications, transport and downhole pipelines and heat exchangers [1]. According to Ref. [2], the global cost caused by corrosion is estimated to be US$2.5 trillion, or 3.4% of the global Gross Domestic Product (GDP) (2013). Among the commonly used solutions to prevent corrosion, namely: the use of steel corrosion inhibitors [3,4], corrosion-resistant alloys [5], or fiber-reinforced plastics [6], employing protective organic coatings represents one of the best approaches in terms of price and final performances [7–9].

Organic coatings are composed of thermosetting resins, mainly thermally cured, solvent-borne, or powder based. Until now, solvent-borne paints have been the most widely used protective coatings for metal because of their high-performances in terms of mechanical properties and ease of application. On the other hand, these paints can cause long-term adverse health effects because of VOCs release and have an inefficient curing process [10,11]. The cross-linking process in these coatings requires long periods and is usually conducted at high temperatures using expensive and energy-consuming ovens [12,13]. In this context, UV-curable coatings represent an optimal solution since they overcome the main drawbacks of thermally cured coatings, obtaining process efficiency through reduced curing time (from hours to seconds), lowering energy consumption, and improving environmental sustainability because of the absence of harmful VOCs in their formulation [14]. Despite their evident advantages, UV-curable coatings have rarely been applied to the inner surfaces of pipelines and narrow geometries due to the dimensional difficulties of bringing a UV source inside these spaces. However, in recent years, the progress of UV LED technology has brought onto the market devices with reduced size and limited heat emission [15,16] that could be used for this purpose. In addition, UV LEDs, compared to standard low-pressure mercury-arc lamps, are a better choice because of their reduced size, improved energy efficiency and safety [17]. UV-LED can also be mounted in arrays providing modularity to the UV source and better control over power and irradiance [18].

Curing the inner surface of a pipe is a dynamic process that requires a UV light source moving inside a cylinder, running the entire length while curing the coating. The movement of the UV source can be defined by a linear translation along the cylinder's longitudinal axis and by a rotation around the same axis. To limit possible oscillation during the linear translation and avoid inaccuracies during the curing process, using a source with a 360° circular light can replace an erratic rotational movement and is a preferred solution. The total amount of energy reaching the paint surface must be accurately tailored based on the paint chemistry to fully cure the paint into a coating with the desired mechanical properties. This energy value is generally called energy dose (J/

* Corresponding author. Department of Industrial Engineering, University of Trento, Trento, Italy.
E-mail address: alessandro.condini-1@unitn.it (A. Condini).

https://doi.org/10.1016/j.optmat.2023.114275
Received 17 May 2023; Received in revised form 6 August 2023; Accepted 18 August 2023

Table 1
Technical characteristics of the SST-10-UV LED [20].

UV LED					
Parameter	Symbol	Value			
Wavelength Range [nm]	λ	365–375	380–390	390–400	400–410
Peak Wavelength [nm]	λ_p	370	385	395	405
Forward Voltage [V]	V_f	3.7	3.4	3.3	3.3
Radiometric Flux [mW]	Φ_{typ}	875	1015	1015	930
Viewing Angle [deg]	$2\Phi_{1/2}$	130	130	130	130

cm^2), defined as the power per unit of surface to be applied for a specific amount of time to provide enough energy to cure a liquid film into a hard coating [19]. If this value is not reached, the final performance of the polymer will be affected, and it is thus of the utmost importance to accurately measure this value spatially during the curing process.

In this study, a UV LED lamp with a 360° radiation emission pattern was developed to cure a photosensitive coating in difficult-to-reach surfaces such as the inner surface of pipelines. In particular, the light source was designed to fit inside pipes with diameters ranging from 40 to 200 mm, the most common dimensions of pipeline used in the oil and gas industry. The radiation wavelength of 395 nm was selected to crosslink the photocurable coating. To allow optimal photopolymerization in all points of the coating, the irradiance pattern of the lamp was evaluated using a software in both the radial and linear coordinates as a function of the LEDs arrangement and the pipe diameter. Once the optimal LED configuration was selected, it was constructed, and the spatial irradiance was measured to validate the simulated irradiance profile.

2. Materials and methods

2.1. Materials

A 1 W power UV LED, SST-10-UV [20] (Table 1), with 395 nm peak wavelength (Luminus Devices Inc, Brussels, Belgium) was chosen as the standard UV LED source for this application. Fig. 1 gives the dimensional features reported by the manufacturer. In particular, the LED is a square of 3.5 × 3.5 mm^2, has a height at the center of 1.3 mm and a viewing angle of 130°.

The printed Circuit Board (PCB) where the UV LEDs were placed was designed using KiCAD®.

To generate a 360° radiation profile, the LED arrays were distributed around a cylindrical support in a configuration where each PCB occupies a side of a polygon. Considering the PCB width to be 4.2 mm, the side of each polygon was set to be constant and equal to 6 mm, and the dimension of the final lamp was calculated accordingly for each configuration analyzed.

Table 2 reports the support characteristics for the analyzed polygons, each defined by the radius of the circumscribed circle (R_{ext}), the radius of the inscribed circle (lr), and the total number of LEDs per lamp, considering each array composed of 20 LEDs.

2.2. UV LED radiation pattern

The irradiance produced by a single LED is defined as the power per unit area incident on the surface to be illuminated by the source and it is usually expressed as $E = d\Phi/dA$ and measured in W/m^2 [21]. The relative intensity of the radiation field around the emission source depends on the viewing angle and, in standard LEDs, is expressed by Lambert's equation:

$$I_\theta = I_0 \cos\theta \quad (1)$$

Table 2
Polygonal geometries and number of LEDs on 16 cm length.

Polygon	R_{ext} [mm]	lr [mm]	n LEDs
Square	4.24	3.00	80
Hexagon	6.00	5.20	120
Octagon	7.84	7.24	160
Decagon	9.71	9.23	200

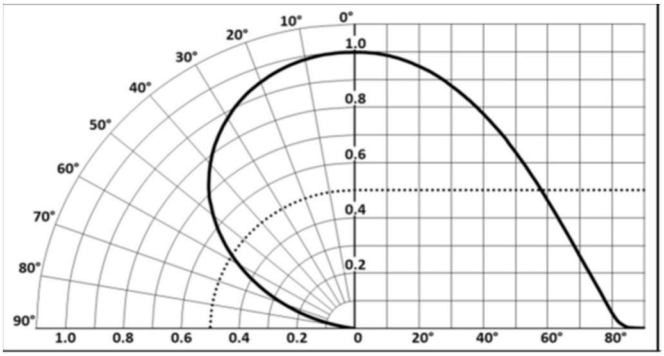

Fig. 2. Radiation pattern of the UV LED, SST-10-UV.

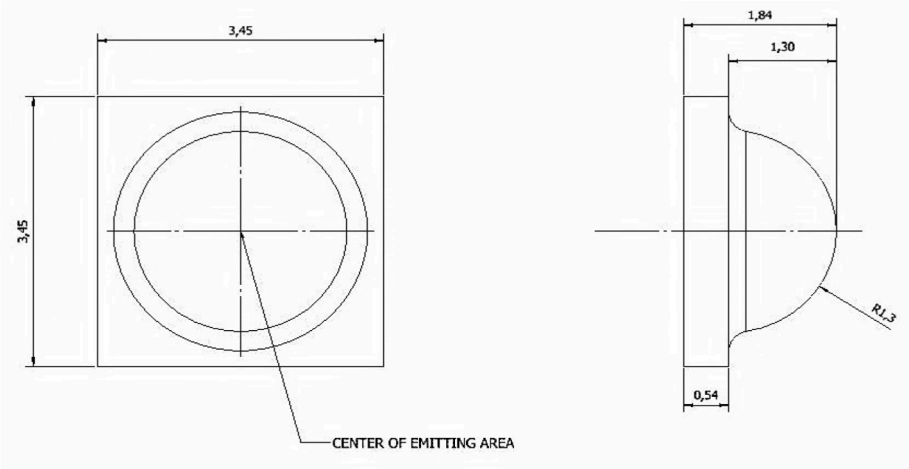

Fig. 1. PDS product data sheet - 002674 luminus devices, inc [20].

Where I_0 is the maximum intensity at the surface normal to the LED, and θ is the viewing angle. The spatial distribution of irradiance obtainable with equation (1) represents the radiation pattern and it is specific for every LED and for this case study is given in Fig. 2. The irradiance distribution (E_θ) can also be expressed as a cosine function according to:

$$E_\theta = \frac{d\Phi}{dA} = \frac{I_0 \cos\theta}{r^2} \quad (2)$$

Where Φ is the radiometric flux, A is the incident area, and r is vthe distance between the viewing point and the source [22]. Considering a system composed of more than one LED, several mathematical models have been reported describing the resulting radiation pattern [21,23,24], but none describing the radiation pattern inside a cylindrical shape. For the polymerization of a coating inside a pipe, the radiating source resulting from the LED arrays disposed around the cylindrical support is required to emit light at 360°. The total radiation pattern is required to be as homogeneous as possible, and it is the result of the combination of the single LEDs radiation patterns in both polar and cartesian coordinates with respect to the lamp axis.

The radiation pattern simulation was performed using the analytical software GNU Octave®. The model developed used the UV LED relative position, viewing angle, radiation pattern, and radiation angle (Fig. 2). Two separate versions of the model were generated. The first one produced a linear profile on a section parallel to the axis of the cylinder, taking as input the number of lined LEDs (n), their relative distance (step), the inner radius of the cylinder to be irradiated (p_r) and the radius of the lamp body (l_r). The second radial, on a section perpendicular to the cylinder's axis, taking as inputs the number of LEDs distributed radially (n) or the number of sides of the polygon, the radius of the cylinder to be irradiated (p_r) and the radius of the lamp body. The models do not consider the contribution of the light reflected by the painted surface of the pipe, as this is considered neglectable.

The total irradiation generated by the lamp was analyzed using a simplified model considering the internal pipe surface as a flat surface. The irradiance distribution, in this case, was evaluated as the total radiometric flux divided by the inner surface of the pipe.

$$E = \frac{\Phi}{A} = \frac{\Phi}{2\pi p_r L} \quad (3)$$

Where E is the irradiance [mW/cm^2], Φ is the total radiant flux of the lamp [W], p_r is the radius of the pipe to be irradiated by the source [mm], and L is the length of the pipe [cm].

A UV radiometer X1-5 equipped with an RCH-119 detector (Gigahertz Optik GmbH, Türkenfeld, Germany) was used to measure the real irradiance after the lamp was constructed. The radiometer measuring device was fixed on a support while the lamp was mounted on a moving rod operated by an inverter motor. A value of irradiance was registered every 4 mm distance for the linear profile or every 10° for the radial profile. The irradiance value for each measurement point was obtained as an average of 3 different results.

3. Results

3.1. Radial radiation patterns

The radial irradiation profiles generated by several lamp geometries were evaluated on a cylindrical surface with an inner radius (p_r) ranging from 10 mm to 100 mm using the simplified model of the flat surface (3). The results, plotted on polar diagrams, show the radial level of irradiation ranging from 0 to 100%. The distance of the light source from the center of the cylinder (l_r) was assumed constant and equal to 7 mm for all polygonal profiles.

Starting with small p_r values, the radial emission diagrams obtained were non-uniform as the radiation intensity oscillated considerably, reaching 100% values only in correspondence with the LED position.

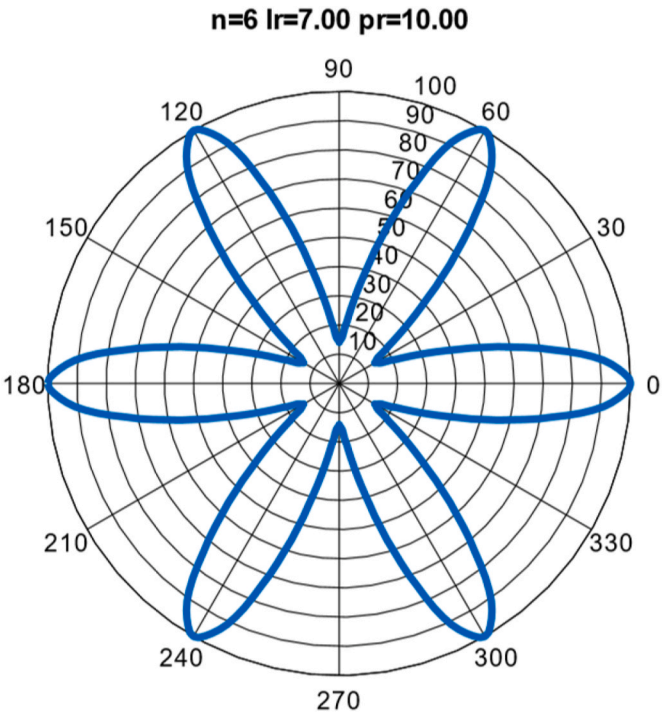

Fig. 3. Radial radiation pattern generated by a hexagonal UV LED source on a cylindrical surface of inner radius p_r = 10 mm.

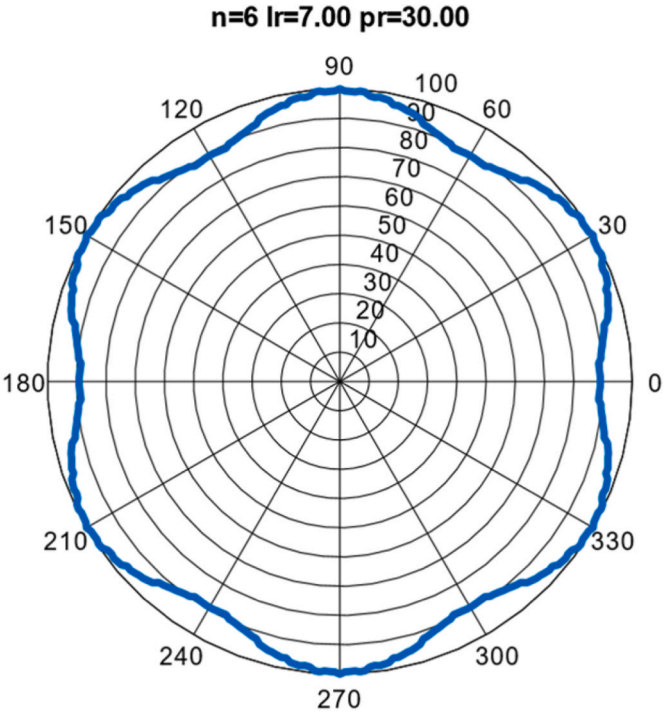

Fig. 4. Radial radiation pattern generated by a hexagonal UV LED source on a cylindrical surface of inner radius p_r = 30 mm.

This can be clearly seen in Fig. 3, where is depicted the radiation pattern generated by a hexagonal lamp on a cylinder with p_r = 10 mm.

When the distance from the source to the surface, given by p_r-l_r is too small, each LED can irradiate only a small portion of the surface immediately in front of it and no side contribution is given to adjacent LEDs.

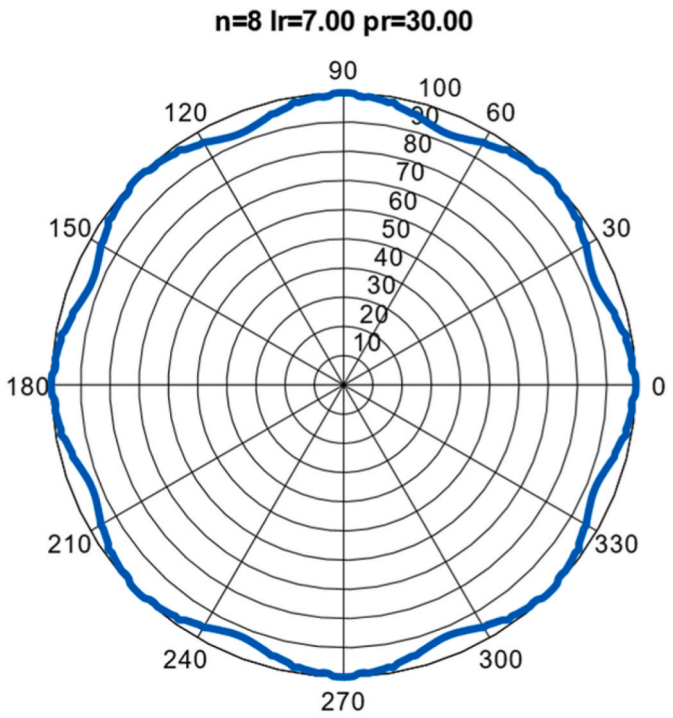

Fig. 5. Radial radiation pattern generated by an octagonal UV LED source on a cylindrical surface of inner radius $p_r = 30$ mm.

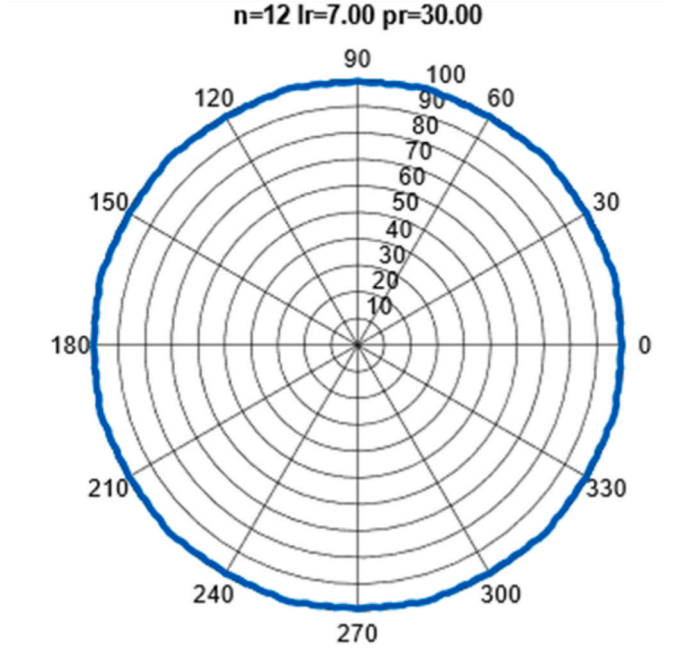

Fig. 6. Radial radiation pattern generated by a dodecagonal UV LED source on a cylindrical surface of inner radius $p_r = 30$ mm.

Considering the same hexagonal source, when the cylinder radius is increased from 10 to 30 mm (Fig. 4), the radiation pattern becomes more evenly distributed on the cylindrical surface, reaching an average level of irradiation of around 95%. Increasing even more the p_r value, the irradiance becomes constant at around 100%, with a profile closer to a circumference.

This tendency is particularly true for lamp geometries with a higher number of sides n. As the distance from the source increases, the contribution of each LED to the adjacent LED emission pattern becomes more critical and the areas where there is no radiation become smaller because of irradiance overlapping.

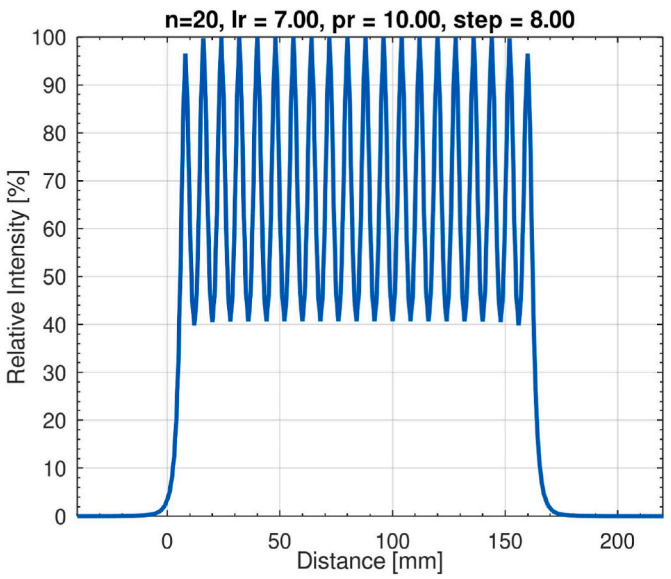

Fig. 7. Linear radiation pattern generated by a hexagonal UV LED source on a cylindrical surface of inner radius $p_r = 10$ mm.

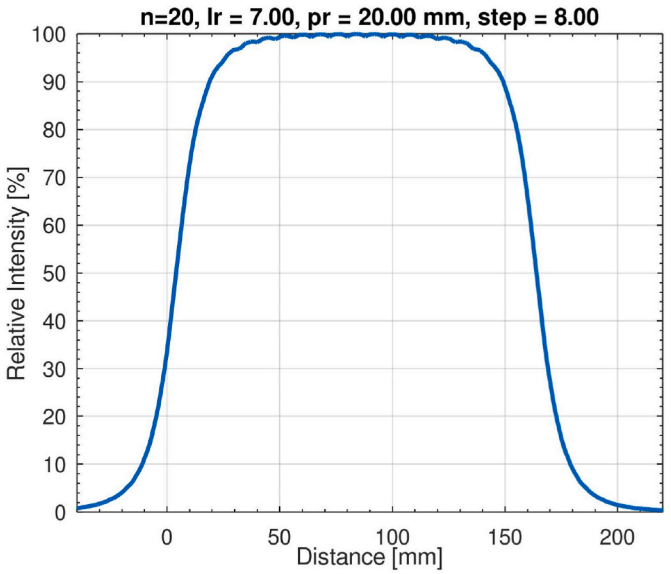

Fig. 8. Linear radiation pattern generated by a hexagonal UV LED source on a cylindrical surface of inner radius $p_r = 20$ mm.

Increasing the number of sides (n) of the light source, the radiant flow remains uniform also inside cylinders of small diameters. This situation is visible in Figs. 5 and 6, where 8- and 10-sided sources ($n = 8$, $n = 10$) irradiate a cylindrical surface diameter of 60 mm (p_r 30 mm) uniformly.

Despite the excellent result in uniformity of the radiant flow, a light source with more than six sides is too large compared to the diameters of the cylinders we want to access, thus limiting the range of cylinders that can be cured.

Therefore, considering the size of the UV LEDs and the dimensional results of the radial radiation analysis, the hexagonal geometry is the suggested source for our purposes.

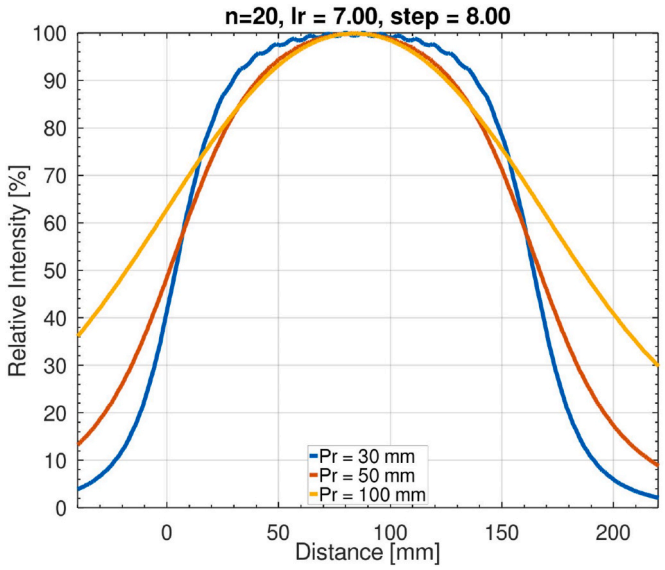

Fig. 9. Linear radiation pattern generated by a hexagonal UV LED source on a cylindrical surface of inner radius p_r = 30, 50 and 100 mm.

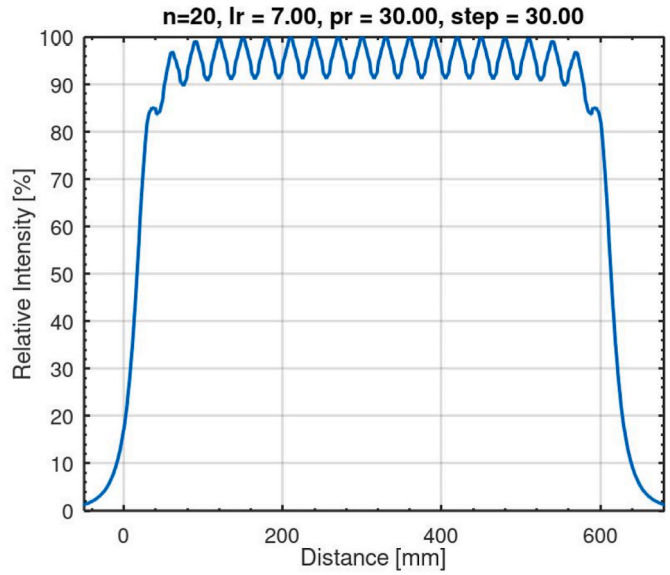

Fig. 10. Linear radiation pattern generated by a hexagonal UV LED source on a cylindrical surface of inner radius p_r = 30 and step = 30 mm.

3.2. Linear radiation patterns

Once the optimal lamp radial configuration was defined, the linear irradiation was analyzed as a function of the step between LEDs and cylinder size. Fig. 7 shows the linear radiation pattern obtained for a hexagonal lamp at a close distance to the cylindrical surface; as expected, at low p_r values, the radiation pattern has no room for overlapping and a discontinuous profile is generated.

The minimum value of p_r at which the linear radiation pattern becomes uniform is 20 mm, corresponding to a cylindrical surface diameter of 40 mm (Fig. 8).

Thus, the higher the p_r values becomes, the lower the oscillations in the linear profile. However, while it is true that increasing the value of p_r generates smother irradiance at the surface, increasing too much this value generates a parabolic shape (Fig. 9).

This effect leads to the fact that the maximum intensity value is maintained for a shorter length compared to cases where the surface to be irradiated is closer to the source. This effect must be taken into consideration when it comes to evaluating the lamp speed along the pipe.

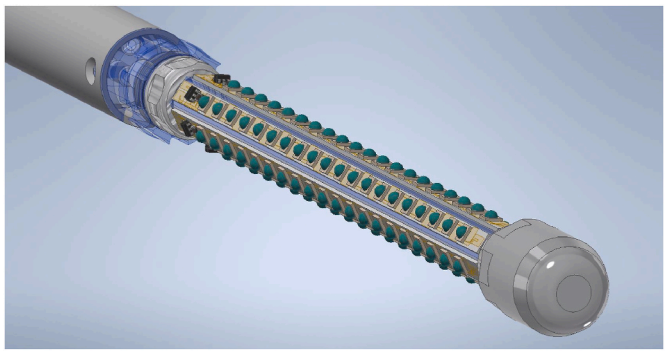

Fig. 11. 3D model of the hexagonal UV LED source constructed.

Table 3
Irradiance values measured with a radiometer at increasing distances from the source.

Distance from LED (d) [mm]	Theoretical I [mW/cm^2]	Measured Irradiance [mW/cm^2]	Abs Error [%]
1	702,5	710.1	1.08
2	442,3	450.5	1.85
3	322,8	328.2	1.68
4	254,1	250.7	1.34
5	209,5	210.0	0.23
6	178,3	175.8	1.37
7	155,1	150.3	3.09
8	137,3	129.8	5.44
9	123,1	120.2	2.37
10	111,6	105.0	5.93

Finally, the effect of changing the distance between LEDs was evaluated. Decreasing the step resulted in a smoother profile with a lobe shape. However, reducing step size means having a shorter lamp and thus, lower movement along the pipe. In addition, increasing the density of LEDs in each array would result in heat dissipation issues. For these reasons, it was not considered to use a step size smaller than 8 mm. On the other hand, the effect of increasing the step on the linear radiation pattern is depicted in Fig. 10.

With a step size of 30 mm, the profile appears less uniform, with an irradiance oscillating between 90 and 100% of the maximum. In this case, the resulting length of the lamp will be increased from 160 mm to 570 mm with a resulting higher lamp speed.

3.3. Irradiance patterns validation

Following the analysis, the UV LED source chosen to continue the experimentation is based on an array of 120 *UV LEDs Luminus SST-10-UV* distributed in 6 strips of 20 LEDs spaced 8 mm apart and fixed on hexagonal aluminum support. Fig. 11 shows the 3D model of the hexagonal UV LED source described. The overall resulting radiant flux is $\Phi = 120$ W, and the achievable irradiation on a cylindrical surface having the same length as the UV LED source is obtained by the following formula:

$$E = \frac{120W}{2\pi P_r \, x \, 16cm} = \frac{1,19}{P_r} \, W \Big/ cm^2 \tag{4}$$

When the inner surface of a cylinder is characterized by a pipe radius (P_r) ranging between 10 mm and 100 mm (meaning a source-surface distance between 3 mm and 93 mm), we obtain irradiation between 1200 mW/cm^2 and 120 mW/cm^2. Consequently, the irradiation needed for the correct UV curing can be tuned by the power of the UV LED.

Larger diameters of the cylinder to be irradiated need more extensive

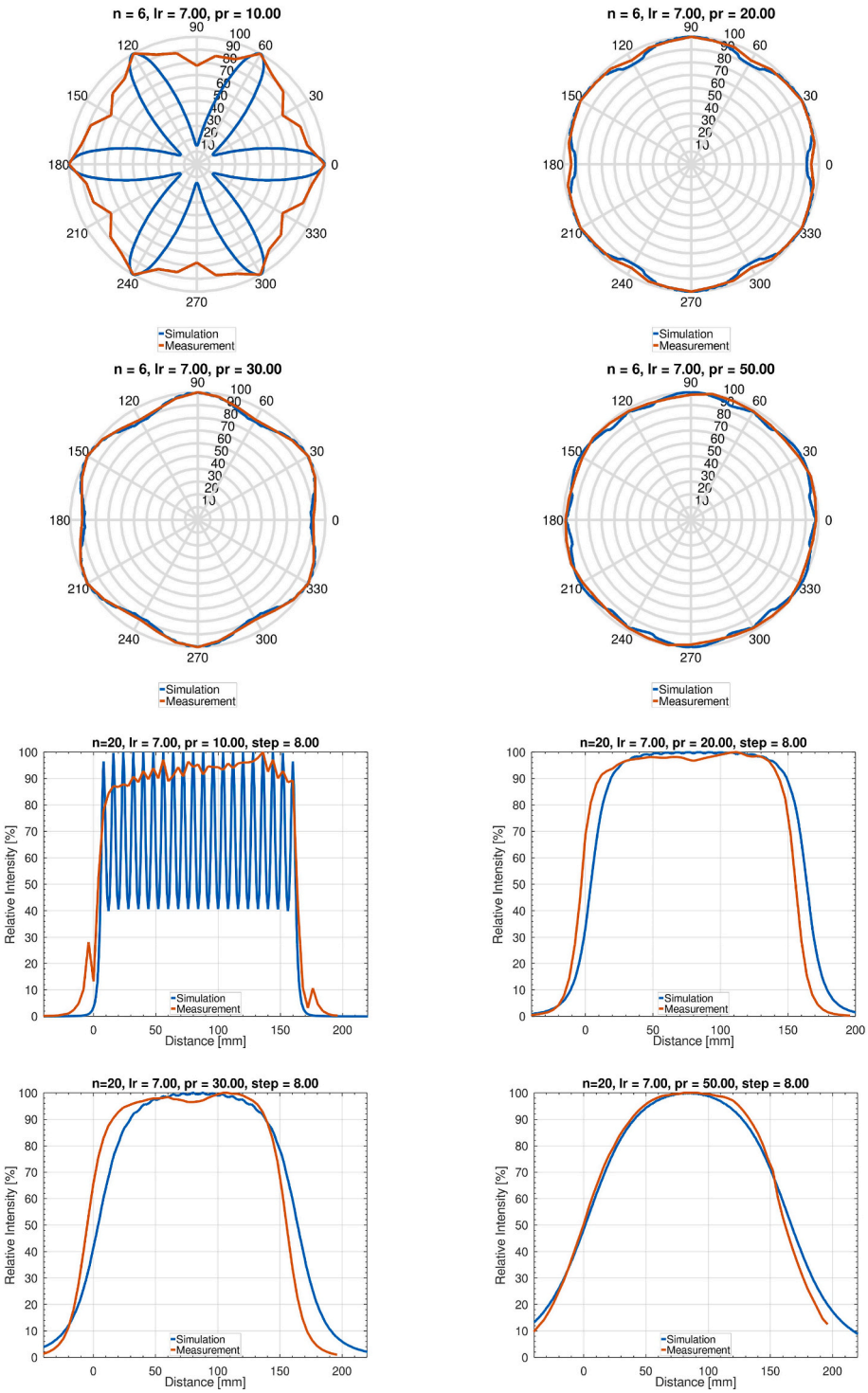

Fig. 12. Comparison between simulated radiation patterns an experimental data for radial (a–d) and linear (e–h) radiation pattterns patterns for different p_r values.

supports, which can be obtained by increasing the number or the dimension of the sides.

The experimental irradiance values were calculated with increasing the distance from the LED source ($d = p_r - l_r$). It was found that the values of intensity registered by the instrument corresponded to the theoretical values obtained with equation (3) with maximum error of less than 6%, which can be ascribed to the operator error in measuring the distance d (Table 3).

Finally, the radial and linear irradiance profiles were evaluated by measuring the intensity values, respectively while rotating and translating the lamp along its axis. Except for the pattern corresponding to p_r value of 10 mm where the collected points were too few to have a reliable curve, all the radiation patterns were found to be consistent with the ones obtained by computer simulation (Fig. 12).

4. Discussion

After the developed model was validated using UV intensity data collected through the radiometer, it was possible to use the simulation to determine the optimal radiation pattern to cure UV paint formulations

applied on the inner surface of different pipe sizes. For each pipe or vessel diameter, it is then possible to choose lamp designs with optimized radiation patterns which have the lowest oscillation in intensity along the whole length of the lamp. Depending on the UV paint formulation chosen for the application, the correct UV intensity (mW/cm2) and dose (J/cm2) required for the correct cure can be easily tailored by acting on the lamp. If a different dose is needed, the lamp speed across the pipe can be increased or decreased. On the other hand, if a different peak intensity is required, the LED current can be increased or decreased to have from 50 to 200% of the nominal power or radiometric flux [20].

A 120 W lamp with a LED array length of 200 mm would require an average of 8.5 min to cure a coating on a 10 m long pipe, with a 10 s dwell time. This time can be easily reduced by half or 4 times by increasing twice or 4 times the lamp length. Depending on the required productivity, several single lamp lines can be used in parallel matching the production obtained by curing the coating with high-temperature ovens with a considerably lower energy consumption.

Despite the high energy efficiency of LED systems, the heat generated by the lamp while in use is an issue that can lead to a critical temperature increase on the PCB chip. This temperature should never surpass the threshold value of 80 °C to avoid consequent reduction of power, LED damage or desoldering [20]. For this reason, a possible solution would be to introduce an internal water cooling system to avoid overheating.

Another common issue arising from using LED units in a chemicals-rich environment is VOC contamination of LED silicon lenses. This contamination is generally caused by the outgassing of adhesives, gaskets or coatings present in close contact with the LED. The VOCs produced this way will penetrate the lens and occupy the free space within the silicone polymer; with subsequent exposure to high photon energy and heat produced by the LED, the volatile compounds trapped will undergo discoloration which will cause the LED to lose intensity [25,26]. To avoid this effect, LEDs must be screened from the VOCs produced from the curing coating with a transparent cover with optimal light transmittance properties (e.g., quartz).

5. Conclusions

In this study, the radiance patterns generated by a modular UV LED lamp for curing UV coatings inside pipelines were presented. The irradiance profiles were evaluated as a function of the number of LEDs and the arrangement along the lamp structure, the LEDs spacing (step) and the distance from the source to the pipe internal surface. The dependence of linear and radial profiles from the aforementioned parameters was evaluated and it was found that a lamp with hexagonal geometry consisting of 6 arrays of 20 LEDs with an 8 mm step between one another was the best configuration to achieve the optimal radiation pattern with the minimum encumbrance. The chosen lamp was then constructed, and the real irradiance was measured using a radiometer at various distances. It was found that both the linear and radial radiation patterns presented the same profile as the one simulated and the irradiance measured as mW/cm^2 was accurate with an error smaller than 6% for all the distances from the source. Therefore, it was demonstrated the possibility to use a modular LED lamp to produce a suitable and uniform radiation pattern to properly cure a UV-curable coating applied on the inner surface of pipes with small diameters.

Despite good validation obtained from intensity measures, the simulation remains an approximation of the intensity of the UV light on a flattened surface. For more complex systems in which different geometries are present (e.g., closed vessels and curved pipes) a more detailed simulation should be preferred to have more accurate patterns. In addition, the values of pipe diameters used in this study cover only a small range of the ones commonly used and with bigger distances from the source to the surface, a different lamp design should be introduced to avoid the intensity of light reaching the coated surface being too low to allow the crosslinking reaction.

CRediT authorship contribution statement

Alessandro Condini: Writing and reviewing. **Viktor Morozov:** Software, and hardware construction. **Carlo Trentalange:** writing, data collection and, Visualization, Validation. **Stefano Rossi:** Supervision, reviewing.

Declaration of competing interest

The authors declare the following financial interests/personal relationships which may be considered as potential competing interests: Alessandro Condini reports financial support and administrative support were provided by Elixe srl and by the public funds of Provincia di Trento, Italy (legge 13 dicembre 1999, n. 6 e ss.mm. “Aiuti per la promozione della ricerca e sviluppo”). Alessandro Condini reports a relationship with Elixe srl that includes: board membership, equity or stocks, and funding grants. Carlo Trentalange reports a relationship with Elixe srl that includes: employment. Co-author Viktor Morozov employer of MPR srl owned by Alessandro Condini.

Data availability

Data will be made available on request.

References

[1] T.E. Perez, Corrosion in the oil and gas industry: an increasing challenge for materials, J. Miner. Met. Mater. Soc. 65 (2013) 1033–1042, https://doi.org/10.1007/s11837-013-0675-3.
[2] NACE international impact, Nace-international-Report, 2023. http://impact.nace.org/documents/Nace-International-Report.pdf. (Accessed 17 April 2023).
[3] M. Askari, M. Aliofkhazraei, R. Jafari, P. Hamghalam, A. Hajizadeh, Downhole corrosion inhibitors for oil and gas production – a review, Applied Surface Science Advances 6 (2021), 100128, https://doi.org/10.1016/j.apsadv.2021.100128.
[4] M.A. Migahed, I.F. Nassar, Corrosion inhibition of Tubing steel during acidization of oil and gas wells, Electrochim. Acta 53 (2008) 2877–2882, https://doi.org/10.1016/j.electacta.2007.10.070.
[5] N. Sridhar, R. Thodla, F. Gui, L. Cao, A. Anderko, Corrosion-resistant alloy testing and selection for oil and gas production, Corrosion Engineering, Sci. Technol. 53 (2017) 1–15, https://doi.org/10.1080/1478422X.2017.1384609.
[6] F.G. Alabtah, E. Mahdi, F.F. Elyian, The use of fiber reinforced polymeric composites in pipelines: a review, Compos. Struct. 276 (2021), 114595, https://doi.org/10.1016/j.compstruct.2021.114595.
[7] L. Fan, S.T. Reis, G. Chen, M.L. Koenigstein, Corrosion resistance of pipeline steel with damaged enamel coating and cathodic protection, Coatings 8 (2018) 185, https://doi.org/10.3390/coatings8050185.
[8] A.K. Hussain, N. Seetharamaiah, M. Pichumani, C.S. Chakra, Research progress in organic zinc rich primer coatings for cathodic protection of metals – a comprehensive review, Prog. Org. Coating 153 (2021), 106040, https://doi.org/10.1016/j.porgcoat.2020.106040.
[9] S. Pourhashem, E. Ghasemy, A. Rashidi, M.R. Vaezi, A review on application of carbon nanostructures as nanofiller in corrosion-resistant organic coatings, J. Coating Technol. Res. 17 (2019) 19–55, https://doi.org/10.1007/s11998-019-00275-6.
[10] M.F. Cunningham, J.D. Campbell, Z. Fu, J. Bohling, J.G. Leroux, W. Mabee, T. Robert, Future Green Chemistry and sustainability needs in polymeric coatings, Green Chem. 21 (2019) 4919–4926, https://doi.org/10.1039/C9GC02462J.
[11] F.D. Dick, Solvent neurotoxicity, Occup. Environ. Med. 63 (2006) 221–226, https://doi.org/10.1136/oem.2005.022400.
[12] C.K. Schoff, Organic Coatings: the paradoxical materials, Prog. Org. Coating 52 (2005) 21–27, https://doi.org/10.1016/j.porgcoat.2004.05.001.
[13] A. Javadi, H.S. Mehr, M. Sobani, M.D. Soucek, Cure-on Command technology: a review of the current State of the art, Prog. Org. Coating 100 (2016) 2–31, https://doi.org/10.1016/j.porgcoat.2016.02.014.
[14] A. Khan, K. Balakrishnan, T. Katona, Ultraviolet light-emitting diodes based on group three nitrides, Nat. Photonics 2 (2008) 77–84, https://doi.org/10.1038/nphoton.2007.293.
[15] D. Li, K. Jiang, K. Sun, C. Guo, AlGaN photonics: recent advances in materials and ultraviolet devices, Adv. Opt Photon 10 (2018) 43–110, https://doi.org/10.1364/AOP.10.000043.
[16] Z. Wang, W.Z. Tang, M. Sillanpää, J. Li, UV Disinfection sensitivity index of spores or protozoa: a model to predict the required fluence of spores or protozoa, Water Sci. Technol. 86 (2022) 2820–2833, https://doi.org/10.2166/wst.2022.391.
[17] C. Dreyer, M. Franziska, Application of LEDs for UV-curing, III-Nitride Ultraviolet Emitters 227 (2016) 415–434, https://doi.org/10.1007/978-3-319-24100-5_15.
[18] R.W. Stowe, Practical aspects of irradiance and energy in UV curing. https://inis.iaea.org/collection/NCLCollectionStore/_Public/31/016/31016357.pdf, 1999.

[19] N. Salleh, N. Ghazali, Y. Mohd, H. Azman, B. Aznizam, M. Munirah, The effect of radiation dosages and UV/EB radiation on the properties of nanocomposite coatings, Int. J. Polym. Mater. 58 (2009) 384–399, https://doi.org/10.1016/j.radphyschem.2010.07.021.
[20] Luminus, Inc., Luminus SST-10-UV, PDS-002674. https://download.luminus.com/datasheets/Luminus_SST-10-UV_Datasheet.pdf, 2021.
[21] I. Moreno, P.X. Viveros-Méndez, Modeling the irradiation pattern of LEDs at short distances, Opt Express 29 (2021) 6845–6853, https://doi.org/10.1364/OE.419428.
[22] Optical modeling for the LED radiation patterns, http://rportal.lib.ntnu.edu.tw:8080/server/api/core/bitstreams/2d2f1c3f-2779-4056-bae9-11567a2860c9/content (accessed 17 April 2023).
[23] I. Moreno, C. Sun, Modeling the irradiation pattern of LEDs, Opt Express 16 (2008) 1808–1819, https://doi.org/10.1364/OE.16.001808.
[24] I. Rachev, T. Djamiykov, M. Marinov, N. Hinov, Improvement of the approximation accuracy of LED radiation patterns, Electronics 8 (2019) 337, https://doi.org/10.3390/electronics8030337.
[25] Cree-LED, XLamp LEDs chemical compatibility. https://assets.cree-led.com/a/da/x/XLamp-Chemical-Compatibility.pdf, 2023.
[26] Luminus, Inc., Guidelines to prevent LED damage due to contamination. https://download.luminus.com/datasheets/APN-002816_Rev01_Guidelines_to_Prevent_LED_Darkening_Due_to_Contamination.pdf, 2021.